AMB Express

ORIGINAL ARTICLE Open Access

# An efficient gene targeting system using Δ*ku80* and functional analysis of Cyp51A in *Trichophyton rubrum*

Masaki Ishii[1*], Tsuyoshi Yamada[2,3] and Shinya Ohata[1*]

**Abstract**

*Trichophyton rubrum* is one of the most frequently isolated fungi in patients with dermatophytosis. Despite its clinical significance, the molecular mechanisms of drug resistance and pathogenicity of *T. rubrum* remain to be elucidated because of the lack of genetic tools, such as efficient gene targeting systems. In this study, we generated a *T. rubrum* strain that lacks the nonhomologous end-joining-related gene *ku80* (Δ*ku80*) and then developed a highly efficient genetic recombination system with gene targeting efficiency that was 46 times higher than that using the wild-type strain. Cyp51A and Cyp51B are 14-α-lanosterol demethylase isozymes in *T. rubrum* that promote ergosterol biosynthesis and are the targets of azole antifungal drugs. The expression of *cyp51A* mRNA was induced by the addition of the azole antifungal drug efinaconazole, whereas no such induction was detected for *cyp51B*, suggesting that Cyp51A functions as an azole-responsive Cyp51 isozyme. To explore the contribution of Cyp51A to susceptibility to azole drugs, the neomycin phosphotransferase (*nptII*) gene cassette was inserted into the *cyp51A* 3′-untranslated region of Δ*ku80* to destabilize the mRNA of *cyp51A*. In this mutant, the induction of *cyp51A* mRNA expression by efinaconazole was diminished. The minimum inhibitory concentration for several azole drugs of this strain was reduced, suggesting that dermatophyte Cyp51A contributes to the tolerance for azole drugs. These findings suggest that an efficient gene targeting system using Δ*ku80* in *T. rubrum* is applicable for analyzing genes encoding drug targets.

**Key Points**

1. A novel gene targeting system using Δ*ku80* strain was established in *T. rubrum*
2. Cyp51A in *T. rubrum* responds to the azole antifungal drug efinaconazole
3. Cyp51A contributes to azole drug tolerance in *T. rubrum*

**Keywords** Dermatophyte, *Trichophyton rubrum*, Ku80, Cyp51A

*Correspondence:
Masaki Ishii
m_ishii@musashino-u.ac.jp
Shinya Ohata
shiohata@musashino-u.ac.jp
[1]Research Institute of Pharmaceutical Sciences, Faculty of Pharmacy, Musashino University, Tokyo 202-8585, Japan
[2]Teikyo University Institute of Medical Mycology, Teikyo University, Hachioji, Tokyo 192-0395, Japan
[3]Asia International Institute of Infectious Disease Control, Teikyo University, Tokyo, Japan

## Introduction

Dermatophytosis is a superficial fungal infection with symptoms such as itching, redness, and nail abnormalities. Tinea pedis (athlete's foot), a type of dermatophytosis, affects approximately 10% of the world's population (Havlickova et al. 2008). *Trichophyton rubrum*, the most common dermatophyte (Zhan and Liu 2017), is a clinically important organism that reduces the quality of life and has a unique life cycle as an anthropophilic dermatophyte that specifically inhabits human surface tissues. A limited class of antifungals, such as azole antifungals, are used in dermatophytosis treatment. Although drug resistance issues in *T. rubrum* have resulted in a need to elucidate the detailed molecular mechanisms of its drug resistance and to identify and analyze drug targets (Yamada et al. 2017; Monod et al. 2019), these issues have not been completely clarified because of the underdevelopment of genetic methods in *T. rubrum*.

Homologous recombination (HR), a repair mechanism for DNA double-strand, is one of the most commonly used genetic engineering methods (Smithies et al. 1985). This technique allows not only the precise insertion of any DNA fragment into the desired genomic region, but also the introduction of mutations, deletions, and replacements based on sequence homology. Nevertheless, eukaryotes also possess a nonhomologous end-joining (NHEJ) repair mechanism for double-strand breaks, which competes with HR-mediated insertion of DNA into target regions (Krappmann 2007). To efficiently promote targeted integration via HR, several fungal species have been engineered by disrupting either of the Ku70/Ku80 complexes involved in NHEJ (Yamada et al. 2009; Matsumoto et al. 2021). These strains have demonstrated the effectiveness of improving HR efficiency in various fungi (Yamada et al. 2009; Matsumoto et al. 2021).

Azole antifungal drugs used for treating dermatophytosis target the lanosterol demethylase Cyp51, which functions in the ergosterol synthesis pathway. XP_003235929 and XP_003236980 in *T. rubrum* have been identified as Cyp51A and Cyp51B homologs, respectively (Celia-Sanchez et al. 2022). It has been reported that the addition of azole antifungal drugs induces fungal Cyp51 expression (Henry et al. 2000; Roundtree et al. 2020). This result suggests that Cyp51A functions as a responsible Cyp51 isozyme when ergosterol biosynthesis is hindered, such as during treatment with azole antifungals. Because the *cyp51* homolog *erg11* is an essential gene in budding yeast (Kalb et al. 1987), a deficiency of dermatophyte *cyp51A* could cause strong growth defects. In budding yeast, disruption of the natural 3′-untranslated region (UTR) by the insertion of an antibiotic-resistant marker was found to destabilize the corresponding mRNAs, and this strategy has been used to analyze essential genes (Schuldiner et al. 2005; Breslow et al. 2008).

In this study, we established a highly efficient HR system using a *ku80*-deficient strain of *T. rubrum* CBS118892 (Martinez et al. 2012), a clinically isolated strain from a patient's nail. This strain has been used for whole genome analysis (Martinez et al. 2012) and several transcriptome analyses (Persinoti et al. 2014; Mendes et al. 2018; Martins et al. 2019; Cao et al. 2022), as well as to produce genetically modified strains (Lang et al. 2020; Ishii et al. 2023, 2024a,b). Therefore, we used this strain as a parent strain of *ku80* deletion strain. Using this established system, we developed a mutant in which the neomycin phosphotransferase (*nptII*) gene was inserted into the 3′-UTR of *cyp51A*, which encodes a target for azole antifungals. When the azole antifungal drug efinaconazole was added, the magnitude of increase in *cyp51A* expression decreased in this mutant, which also exhibited sensitivity to ravuconazole and efinaconazole. This study would accelerate the production of genetically engineered strains to investigate the pathogenicity and drug resistance of *T. rubrum* and provide novel insights into antifungal targets.

## Materials and methods

### Fungal and bacterial strains and culture conditions

*Trichophyton rubrum* CBS118892 was cultured on Sabouraud dextrose agar (SDA; 1% Bacto peptone, 4% glucose, 1.5% agar, pH unadjusted) at 28 °C. The conidia of *T. rubrum* were prepared as described previously (Uchida et al. 2003). We confirmed the sequence of *cyp51A* and *cyp51B* as well as their promoters and terminators.

### Plasmid construction

To construct a *ku80*-targeting vector, pAg1-Δ*ku80-flp*, approximately 2.1 and 1.5 kb of the 5′- and 3′-UTR fragments, respectively, of the *ku80* open reading frame (ORF) were amplified from *T. rubrum* genomic DNA by polymerase chain reaction (PCR). The PCR products of the 5′- and 3′-UTR fragments were cleaved by *Spe*I/*Apa*I and *Bgl*II/*Kpn*I, respectively. The plasmid backbone of pAg1 (Zhang et al. 2003) and the FLP/FRT module (Reuß et al. 2004) of pMRV-TmKu80/T2 were cleaved by *Spe*I/*Kpn*I and *Apa*I/*Bam*HI, respectively (Yamada et al. 2014). These fragments were joined using Ligation high version 2 (TOYOBO, Osaka, Japan). To construct a *cyp51A* 3′-UTR-targeting vector, pAg1-*cyp51A*-3′-UTR, 1.6 kbp of the *cyp51A* ORF and 1.5 kbp of the 3′-UTR fragment of *cyp51* ORF were amplified from *T. rubrum* genomic DNA by PCR. The neomycin phosphotransferase gene cassette, which consists of *E. coli* neomycin phosphotransferase gene (*nptII*), *Aspergillus nidulans trpC* promoter (P*trpC*), and *Aspergillus fumigatus cgrA* terminator (T*cgrA*), was cleaved from pMRV-TmKu80/T2 using *Apa*I and *Cla*I. These fragments were joined using an In-Fusion HD Cloning Kit (TaKaRa Bio, Shiga,

Japan). The primers used in this study are shown in Table 1.

### Transformation of *T. rubrum*

*Trichophyton rubrum* was transformed using the polyethylene glycol (PEG) method as described previously (Yamada et al. 2008). The desired transformants and purified genomic DNA were analyzed by PCR. The *ku80* ORF was replaced with a cassette with the *nptII* and the flippase gene (*flp*) flanked by flippase recognition sequences (Fig. 1a). As *flp* was inserted downstream of the copper ion-responsive promoter $P_{ctr4}$, *nptII* and *flp* were removed from the *ku80*-deficient genome by adding the copper ion chelator bathocuproinedisulfonic acid to induce FLP recombinase expression (Fig. 1a). Total DNA was extracted using the Quick-DNA Fungal/Bacterial Miniprep Kit (Zymo Research, Irvine, USA). Fungal cells were disrupted by μT-01 (TAITEC, Saitama, Japan) using 5-mm stainless beads.

### Antifungal susceptibility assay

Conidia ($2\times10^3$) were incubated with two-fold serial dilutions of antifungal agents in 200 μl 3-Morpholinopropanesulfonic acid (MOPS)-buffered Roswell Park Memorial Institute (RPMI)1640 medium (pH 7.0) at 28 °C for 7 days, and the minimum inhibitory concentration $MIC_{100}$ (minimal concentration required to inhibit growth by 100%) was determined. Efinaconazole was purchased from BLD Pharmatech Ltd, Shanghai, China, and ravuconazole was purchased from Merck, Darmstadt, Germany.

**Table 1** Primers used in this study

| Primer name | Sequences |
|---|---|
| *ku80*-5′-F-*Spe*I | 5′-CGC ACT AGT CCA CTG GAG ATC CCC AAC AG-3′ |
| *ku80*-5′-R-*Apa*I | 5′-CGC GGG CCC TCG GGT CAA ACA GCC ACA AT-3′ |
| *ku80*-3′-F-*Bgl*II | 5′-CGC AGA TCT GCT GCT GGT GGG TAT GTA GG-3′ |
| *ku80*-3′-R-*Kpn*I | 5′-CGC GGT ACC TTC GTT TGA GCC GAG AGA CC-3′ |
| *cyp51A*-F-*Spe*I | 5′-ACT AGT ATG GCC GTG CTC ACA GTG-3′ |
| *cyp51A*-R-*Apa*I | 5′-GGG CCC TAA CGT GAA TTA GAA CGT CGT TC-3′ |
| *cyp51A*-3′-F-*Cla*I | 5′-CGA TCG ATA CTC ACA GTT ATT GAA CAG TTT CTG TA-3′ |
| *cyp51A*-3′-R-*Kpn*I | 5′-GCG GGT ACC AGC TCG GAA ATG CCT TGA CA-3′ |
| Primer 1 | 5′-TGA GGA AGG CCA GGG GAA CTT AT-3′ |
| Primer 2 | 5′-CCT TCC TGC TCT TTG CTT TCC CT-3′ |
| Primer 3 | 5′-AGC TGG TCT CGG AAA GTT GG-3′ |
| Primer 4 | 5′-AAG CCA CCA AAG CTC TCT CC-3′ |
| Primer 5 | 5′-AGC TCC TTC AAT TGA CCC GG-3′ |
| Primer 6 | 5′-AGA TGA TTC ATG ACG TAT ATT CAC CG-3′ |
| Primer 7 | 5′-GAT GGA TTG CAC GCA GGT TC-3′ |
| Primer 8 | 5′-CAC TGT TTT CTG GAC CTA TGA AAC C-3′ |
| Primer 9 | 5′-GCG AAT ACA GCA GAG AGA AAA TTG A-3′ |
| *chs1*-RT-F | 5′-GGC CAC AAC GAA GCC TAT GA-3′ |
| *chs1*-RT-R | 5′-GCT GGG AGG TAC TGT TTG ATC AA-3′ |
| *cyp51A*-RT-F | 5′-CAA TCG GCC TGG GAG ATG-3′ |
| *cyp51A*-RT-R | 5′-TTG GAC TTA GCT CCT TCG CG-3′ |
| *cyp51B*-RT-F | 5′-GAA CAA CGT TGG TGT CAC CG-3′ |
| *cyp51B*-RT-R | 5′-ACA TCT GTG TCT GCC TGA GC-3′ |

### Quantitative reverse transcription-PCR (qRT-PCR)

Total RNAs were purified using NucleoSpin RNA (Macherey–Nagel, Düren, Germany) and reverse-transcribed into cDNAs using ReverTra Ace (Toyobo, Osaka, Japan) according to the manufacturers' instructions. qRT-PCR was performed using TB Green Premix Ex Taq II (TaKaRa Bio, Shiga, Japan) on a StepOne Real-time PCR (Thermo Fisher Scientific, Waltham, USA). The relative mRNA expression level was determined using the $2^{-\Delta\Delta Ct}$*csh1*) as an endogenous control to normalize the samples (Jacob et al. 2012). The primers used in this study are listed in Table 1.

### Statistical analysis

Mean values of three or more groups with two variables were compared using two-way ANOVA with Šidák correction and Tukey's post hoc test, according to the recommendation of Prism 10 (GraphPad, Boston, USA). The difference in the efficiency of HR in wild-type (WT) and Δ*ku80* strains was analyzed by two-sided Fisher's exact test using Prism 10 (GraphPad, Boston, USA). Differences were considered significant at $P<0.05$.

## Results

To increase gene targeting efficiency, we attempted to delete the gene encoding Ku80. WT strain was transformed using the disruption cassette and 14 of the 261 transformants obtained (5.4%) were found to be deficient in *ku80* gene. The cloned fungi were cultivated under conditions in which bathocuproinedisulfonic acid was incorporated into the medium to induce FLP recombinase and facilitate the removal of the *nptII* gene cassette. Subsequent cloning was performed to obtain the deficient strain candidates. To confirm that the *ku80*-deficient strain (Δ*ku80*) was generated as designed, PCR was performed using genomic DNA purified from WT and Δ*ku80* strains (Fig. 1a, top and bottom, respectively) as templates. PCR performed using WT genomic DNA and primers designed for the 5′- and 3′-UTR of *ku80* (Primers 1 and 2 in Fig. 1a, respectively) amplified the PCR products with the expected size (6.6 kbp; Fig. 1b, left lane). The size of PCR products in Δ*ku80* was reduced as expected (3.8 kbp; Fig. 1b, right lane). In contrast, PCR performed using primers designed against sequences in the 5′-UTR (Primer 3 in Fig. 1a) and the ORF of *ku80*

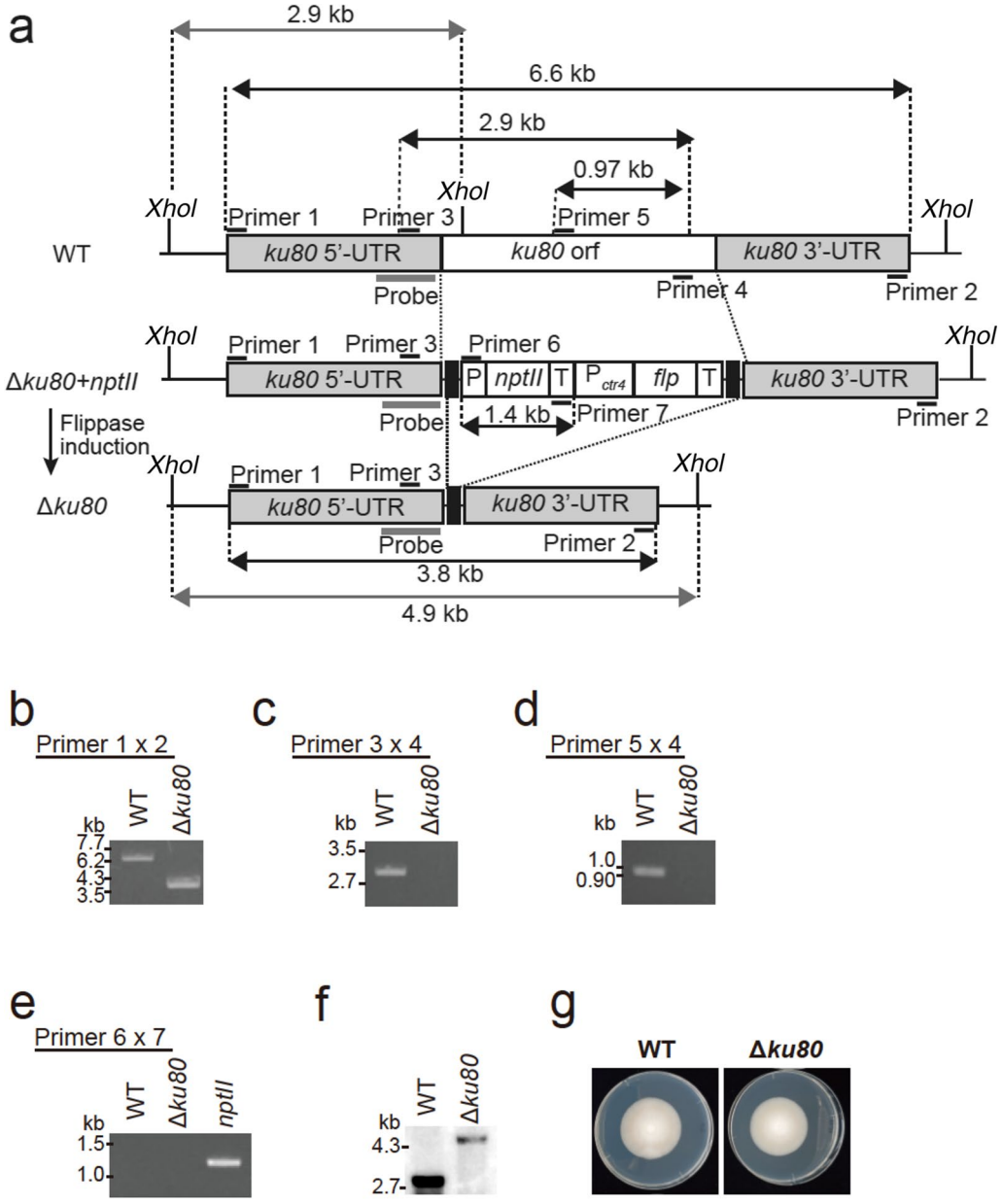


**Fig. 1** *ku80* locus targeting and *nptII* marker excision. **a** Schematic representation of the *ku80* locus before and after excision of the copper ion-responsive promoter $P_{ctr4}$, *nptII* and *flp* in *T. rubrum*. Site-specific recombination between the flanking FRT sequences (black box) was performed by the conditional expression of *flp*. **b**–**e** PCR analysis of total DNA samples from transformants. WT was used as a control. **b** Fragments were amplified with primer pairs (Primers 1 and 2). **c** Fragments were amplified with primer pairs (Primers 3 and 4). **d** Internal fragments of the *ku80* ORF were amplified with primer pairs (Primers 5 and 4). **e** Internal fragments of *nptII* were amplified with primer pairs (Primers 6 and 7). The *nptII*-harboring strain (Δ*cla4*) was used as a positive control. **f** Southern blot analysis of genome DNA samples from wild-type and Δ*ku80* strains. **g** Mycelial growth of WT and Δ*ku80* strains on SDA at 28 °C for 16 days

(Primers 4 and 5 in Fig. 1a) yielded PCR products of the expected size for WT (Fig. 1c, d, left lanes) but not for Δ*ku80* (Fig. 1c, d, right lanes) strain. The deletion of *nptII* from the genome of Δ*ku80*+*nptII* strain (Fig. 1a, middle) was confirmed by PCR using primers designed against the sequences in the promoter and terminator of *nptII* (Primers 6 and 7 in Fig. 1a, respectively, Fig. 1e). The deletion of Δ*ku80* was also confirmed by Southern blot analysis of genomic DNA from WT and Δ*ku80* strains (Fig. 1f). These data indicated that the Δ*ku80* strain was successfully generated with no reduction in the number of available drug markers. To ascertain the extent of the impact of Ku80 protein on growth, we compared mycelial growth between WT and Δ*ku80* strains, which revealed comparable mycelial growth (Fig. 1g).

The mRNA expression of *cyp51A* in *T. rubrum* was upregulated by the addition of the azole antifungal drug efinaconazole, but that of *cyp51B* was not upregulated (Fig. 2a). We attempted to insert the *nptII* cassette into the downstream of *cyp51A* ORF of *T. rubrum*, as demonstrated in budding yeast studies (Schuldiner et al. 2005; Breslow et al. 2008). Using the obtained Δ*ku80* strain, we inserted the *nptII* cassette into *cyp51A* 3′-UTR (hereinafter termed the insertional mutant; Fig. 2b, c). Homologous recombinant strains were obtained in 12 of 26 strains (46.2%; Table 2) in which the insertion of the drug resistance gene within target region was confirmed by PCR using primers designed within the ORF and 3′-UTR of *cyp51A* (Primers 8 and 9, respectively; Fig. 2b, c). The HR efficiency of the Δ*ku80* strain was 46 times higher than that of the WT strain (1/98; 1.0%; Table 2). These data demonstrated that a highly efficient HR method had been established in *T. rubrum*.

Under efinaconazole-free conditions, the mRNA level of *cyp51A* in the two independently isolated insertional mutants, which were derived from the Δ*ku80* strain, were comparable to that in the parent strain Δ*ku80* (Fig. 2d). Nevertheless, efinaconazole-induced elevation of *cyp51A* mRNA level decreased in the insertional mutants (Fig. 2d). These findings suggest that the insertion of the nptII gene cassette into the 3′-UTR of cyp51A causes mRNA perturbation at least under the condition of *cyp51A* induction in *T. rubrum*. The insertional mutants exhibited similar mycelial growth as that of the parent strain Δ*ku80* (Fig. 2e), but it showed increased sensitivity to the azole antifungals efinaconazole and ravuconazole (Table 3). However, the MICs of itraconazole and luliconazole remained unchanged in the insertional mutants. These findings suggest that Cyp51A functions as a factor for azole antifungal tolerance in *T. rubrum*.

## Discussion

*Trichophyton rubrum* is an anthropophilic dermatophyte specialized for human parasitism, whereas several other dermatophytes are zoophilic or geophilic (Reiss Errol et al. 2011). The nature of this fungus is of great interest from not only a medical but also biological point of view. In recent years, transcriptomic, proteomic, and immunological studies of this fungus have been conducted extensively (Xu et al. 2018, 2022; Burstein et al. 2020; Peres et al. 2022; Galvão-Rocha et al. 2023). Nevertheless, molecular and cellular biological studies of *T. rubrum* have been limited partially due to a lack of genetic tools for this organism. In this study, we generated a *ku80*-deficient strain of this fungus and demonstrated that this strain can be applied in efficient HR methods, similar to a system established in a zoophilic dermatophyte, *Trichophyton mentagrophytes* (formerly *Arthroderma vanbreuseghemii*) (Yamada et al. 2009). The method established in this study might serve as a fundamental technique to promote research that will advance the findings of previous comprehensive analyses and immunological analyses observed on the host side.

The insertional mutant, in which the expression induction of *cyp51A* by efinaconazole was attenuated, exhibited increased sensitivity to efinaconazole and ravuconazole. Considering that *cyp51A* expression was upregulated in response to efinaconazole addition, we speculated that *T. rubrum* Cyp51A is an inducible Cyp51 isozyme crucial for tolerance to azole antifungals. Indeed, it has been reported that itraconazole treatment also induces an increase in *cyp51A* expression (Diao et al. 2009). In *A. fumigatus*, loss or suppression of *cyp51A* expression enhances sensitivity to the azole antifungal fluconazole (Hu et al. 2007). Conversely, *cyp51B* deficiency does not significantly alter fluconazole sensitivity (Hu et al. 2007). This difference may be partially explained by the lower binding affinity of Cyp51A for fluconazole than for Cyp51B (Andrew et al. 2010). Nevertheless, a difference in the induction of the expression of each *cyp51* gene in response to azoles may also contribute to this disparity in sensitivity. Regarding *T. rubrum*, no studies have investigated the contribution of Cyp51A and Cyp51B isozymes to the resistance to azole antifungal drugs. It has been reported that strains of *T. mentagrophytes* with a deficiency in Cyp51B exhibit a 2–3-fold reduction in MICs and enhanced susceptibility to itraconazole and voriconazole (Yamada et al. 2022). This observation highlights the necessity for further investigation into the susceptibility of the Cyp51 isozymes in dermatophytes to azole drugs. In the future, it is important to generate *T. rubrum* strains that are deficient in *cyp51A* and *cyp51B*, followed by analyzing their involvement in growth and resistance to azole antifungal drugs.

The induction of Cyp51 expression has been extensively studied in *Aspergillus* species. It is known that in response to ergosterol depletion by azole treatment, the membrane-bound transcription factor SrbA is cleaved by proteases and activated (Dhingra et al. 2016; Bat-Ochir et al. 2016), translocating into the nucleus and upregulating the expression of enzymes involved in the ergosterol synthesis pathway, including Cyp51A (Zhang et al. 2021). A deficiency in SrbA in *A. fumigatus* has been demonstrated to markedly enhance the azole susceptibility of the azole-sensitive and -resistant fungi (Willger et al. 2008; Hagiwara et al. 2016). Moreover, the SrbA-binding region located upstream of the *cyp51A* gene has been shown to contribute to drug resistance by forming tandem repeats (Gsaller et al. 2016; Kühbacher et al. 2022). As the regulatory mechanism of *cyp51* expression in *T. rubrum* is anticipated to represent a novel drug target for azole drug susceptibility and a cornerstone of research for elucidating the mechanism of azole

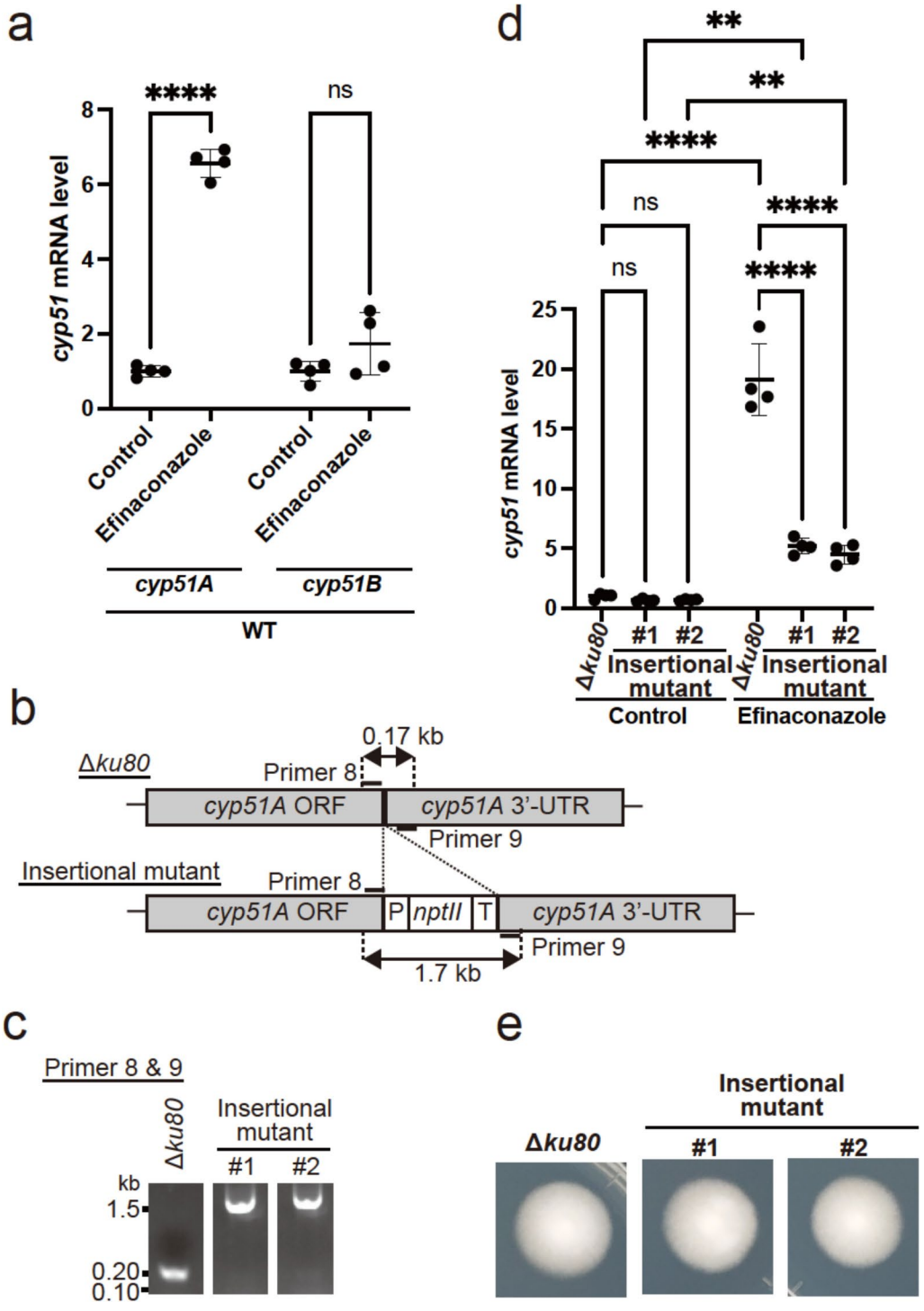


**Fig. 2** Production and characterization of the *cyp51A* 3′-UTR insertional mutants of *T. rubrum*. **a** The mRNA expression of *cyp51A* and *cyp51B* with or without 1 ng/ml efinaconazole in WT. Data are expressed as mean ± SD. The dots on the graph represent biological replicates (n = 4). n.s., not significant. ****, $P < 0.0001$. Two variables were compared using two-way ANOVA with Šidák correction. **b** Schematic representation of the *cyp51A* locus of WT and insertional mutant. **c** PCR analysis of total DNA samples from the independently isolated insertional mutant #1 and #2. The fragments were amplified with primer pairs (Primer 8 and 9). Δ*ku80* was used as a control. **d** The mRNA expression of *cyp51A* in Δ*ku80* and insertional mutant #1 and #2 with or without 1 ng/ml efinaconazole. The bars represent the standard deviation of the data obtained from three independent experiments. Data are expressed as mean ± SD. The dots on the graph represent biological replicates (n = 4–10). n.s., not significant. ****, $P < 0.0001$. Two variables were compared using two-way ANOVA with Tukey's post hoc test. (e) Mycelial growth of Δ*ku80* and insertional mutant #1 and #2 on SDA at 28℃ for 13 days

**Table 2** Gene targeting efficiency of WT and Δ*ku80* strains

| Strain | Total transformants | Homologous replacement | Efficiency (%) |
|---|---|---|---|
| WT | 98 | 1 | 1.0 |
| Δ*ku80* | 26 | 12 | 46.2 |

In homologous replacement cells, the drug resistance gene was inserted between the ORF and 3′-UTR of *cyp51A*. Two-sided Fisher's exact test, $P < 0.0001$

**Table 3** MIC values (μg/ml) of efinaconazole and ravuconazole

| Azole drugs | WT | Δ*ku80* (Parent strain) | Insertional mutant #1 | Insertional mutant #2 |
|---|---|---|---|---|
| Efinaconazole | 0.02 | 0.02 | 0.005 | 0.005 |
| Ravuconazole | 0.08 | 0.08 | 0.04 | 0.04 |
| Itraconazole | 1 | 1 | 1 | 1 |
| Luliconazole | 0.00063 | 0.00063 | 0.00063 | 0.00063 |

Two biological repeats were performed

resistance. Consequently, it is of great interest to elucidate the detailed molecular mechanism of the regulation of *cyp51A* expression by utilizing genetic tools, such as Δ*ku80*, which can be employed to elucidate the molecular mechanisms underlying the regulation of *cyp51A* expression in *T. rubrum*.

#### Abbreviations

| | |
|---|---|
| HR | Homologous recombination |
| MOPS | 3-Morpholinopropanesulfonic acid |
| NHEJ | Nonhomologous end-joining |
| ORF | Open reading frame |
| PEG | Polyethylene glycol |
| PCR | Polymerase chain reaction |
| RPMI | Roswell Park Memorial Institute |
| SDA | Sabouraud dextrose agar |
| UTR | Untranslated region |

#### Acknowledgements
The authors thank H. Uga, N. Hori, H. Hamanaka for their technical help. This work was supported by the Japan Society for the Promotion of Science.

#### Author contributions
MI conceived and designed research. MI conducted experiments. MI, TY and SO analyzed data. MI, TY and SO wrote the manuscript. All authors read and approved the manuscript.

#### Funding
This work was supported by the Japan Society for the Promotion of Science (Grant numbers 23K06533 and 21K15438) and funding from Nihon Nohyaku Co., Ltd..

#### Availability of data and materials
The data that support the findings of this study are available from the corresponding author upon reasonable request.

## Declarations

#### Ethics approval and consent to participate
Not applicable.

#### Consent for publication
Not applicable.

#### Competing interests
Authors have no competing interests.

Received: 25 July 2024 / Accepted: 14 August 2024
Published online: 31 August 2024

#### References

Andrew SWG, Melo N, Martel MC, Parker EJ, Nes DW, Kelly LS, Kelly ED (2010) Expression, purification, and characterization of *Aspergillus fumigatus* sterol 14-α demethylase (CYP51) isoenzymes A and B. Antimicrob Agents Chemother 54:4225–4234. https://doi.org/10.1128/aac.00316-10

Bat-Ochir C, Kwak J-Y, Koh S-K, Jeon M-H, Chung D, Lee Y-W, Chae S-K (2016) The signal peptide peptidase SppA is involved in sterol regulatory element-binding protein cleavage and hypoxia adaptation in *Aspergillus nidulans*. Mol Microbiol 100:635–655. https://doi.org/10.1111/mmi.13341

Breslow DK, Cameron DM, Collins SR, Schuldiner M, Stewart-Ornstein J, Newman HW, Braun S, Madhani HD, Krogan NJ, Weissman JS (2008) A comprehensive strategy enabling high-resolution functional analysis of the yeast genome. Nat Methods 5:711–718. https://doi.org/10.1038/nmeth.1234

Burstein VL, Beccacece I, Guasconi L, Mena CJ, Cervi L, Chiapello LS (2020) Skin immunity to dermatophytes: from experimental infection models to human disease. Front Immunol 11:605644. https://doi.org/10.3389/fimmu.2020.605644

Cao X, Xu X, Dong J, Xue Y, Sun L, Zhu Y, Liu T, Jin Q (2022) Genome-wide identification and functional analysis of circRNAs in *Trichophyton rubrum* conidial and mycelial stages. BMC Genomics 23:21. https://doi.org/10.1186/s12864-021-08184-y

Celia-Sanchez BN, Mangum B, Brewer M, Momany M (2022) Analysis of Cyp51 protein sequences shows 4 major Cyp51 gene family groups across fungi. G3 Genes Genomes Genetics 12:249. https://doi.org/10.1093/g3journal/jkac249

Dhingra S, Kowalski CH, Thammahong A, Beattie SR, Bultman KM, Cramer RA (2016) RbdB, a rhomboid protease critical for SREBP activation and virulence in *Aspergillus fumigatus*. mSphere. https://doi.org/10.1128/msphere.00035-16

Diao Y, Zhao R, Deng X, Leng W, Peng J, Jin Q (2009) Transcriptional profiles of *Trichophyton rubrum* in response to itraconazole. Med Mycol 47:237–247. https://doi.org/10.1080/13693780802227308

Galvão-Rocha FM, Rocha CHL, Martins MP, Sanches PR, Bitencourt TA, Sachs MS, Martinez-Rossi NM, Rossi A (2023) The antidepressant sertraline affects cell signaling and metabolism in *Trichophyton rubrum*. J Fungi. https://doi.org/10.3390/jof9020275

Gsaller F, Hortschansky P, Furukawa T, Carr PD, Rash B, Capilla J, Müller C, Bracher F, Bowyer P, Haas H, Brakhage AA, Bromley MJ (2016) Sterol biosynthesis and azole tolerance Is governed by the opposing actions of SrbA and the CCAAT binding complex. PLoS Pathog 12:e1005775

Hagiwara D, Watanabe A, Kamei K (2016) Sensitisation of an azole-resistant *Aspergillus fumigatus* strain containing the Cyp51A-related mutation by deleting the SrbA gene. Sci Rep 6:38833. https://doi.org/10.1038/srep38833

Havlickova B, Czaika VA, Friedrich M (2008) Epidemiological trends in skin mycoses worldwide. Mycoses 51:2–15. https://doi.org/10.1111/j.1439-0507.2008.01606.x

Henry WK, Nickels TJ, Edlind DT (2000) Upregulation of ERG genes in *Candida* species by azoles and other sterol biosynthesis Inhibitors. Antimicrob Agents Chemother 44:2693–2700. https://doi.org/10.1128/aac.44.10.2693-2700.2000

Hu W, Sillaots S, Lemieux S, Davison J, Kauffman S, Breton A, Linteau A, Xin C, Bowman J, Becker J, Jiang B, Roemer T (2007) Essential gene identification and drug target prioritization in *Aspergillus fumigatus*. PLoS Pathog 3:e24

Ishii M, Matsumoto Y, Yamada T, Uga H, Katada T, Ohata S (2023) TrCla4 promotes actin polymerization at the hyphal tip and mycelial growth in *Trichophyton rubrum*. Microbiol Spectr. https://doi.org/10.1128/spectrum.02923-23

Ishii M, Matsumoto Y, Yamada T, Uga H, Katada T, Ohata S (2024a) Targeting dermatophyte Cdc42 and Rac GTPase signaling to hinder hyphal elongation and virulence. iScience 27:110139. https://doi.org/10.1016/j.isci.2024.110139

Ishii M, Yamada T, Ishikawa K, Ichinose K, Monod M, Ohata S (2024b) The Ptk2-Pma1 pathway enhances tolerance to terbinafine in *Trichophyton rubrum*. Antimicrob Agents Chemother 68:e01609-e1623. https://doi.org/10.1128/aac.01609-23

Jacob TR, Peres NTA, Persinoti GF, Silva LG, Mazucato M, Rossi A, Martinez-Rossi NM (2012) *rpb2* is a reliable reference gene for quantitative gene expression analysis in the dermatophyte *Trichophyton rubrum*. Med Mycol 50:368–377. https://doi.org/10.3109/13693786.2011.616230

Kalb VF, Woods CW, Turi TG, Dey CR, Sutter TR, Loper JC (1987) Primary structure of the P450 lanosterol demethylase gene from *Saccharomyces cerevisiae*. DNA 6:529–537. https://doi.org/10.1089/dna.1987.6.529

Krappmann S (2007) Gene targeting in filamentous fungi: the benefits of impaired repair. Fungal Biol Rev 21:25–29. https://doi.org/10.1016/j.fbr.2007.02.004

Kühbacher A, Peiffer M, Hortschansky P, Merschak P, Bromley MJ, Haas H, Brakhage AA, Gsaller F (2022) Azole resistance-associated regulatory motifs within the promoter of *cyp51A* in *Aspergillus fumigatus*. Microbiol Spectr 10:e01209-e1222. https://doi.org/10.1128/spectrum.01209-22

Lang EAS, Bitencourt TA, Peres NTA, Lopes L, Silva LG, Cazzaniga RA, Rossi A, Martinez-Rossi NM (2020) The *stuA* gene controls development, adaptation, stress tolerance, and virulence of the dermatophyte *Trichophyton rubrum*. Microbiol Res 241:126592. https://doi.org/10.1016/j.micres.2020.126592

Martinez DA, Oliver BG, Gräser Y, Goldberg JM, Li W, Martinez-Rossi NM, Monod M, Shelest E, Barton RC, Birch E, Brakhage AA, Chen Z, Gurr SJ, Heiman D, Heitman J, Kosti I, Rossi A, Saif S, Samalova M, Saunders CW, Shea T, Summerbell RC, Xu J, Young S, Zeng Q, Birren BW, Cuomo CA, White TC (2012) Comparative genome analysis of *Trichophyton rubrum* and related dermatophytes reveals candidate genes involved in infection. Mbio 3:e00259-e312. https://doi.org/10.1128/mBio.00259-12

Martins MP, Silva LG, Rossi A, Sanches PR, Souza LDR, Martinez-Rossi NM (2019) Global analysis of cell wall genes revealed putative virulence factors in the dermatophyte *Trichophyton rubrum*. Front Microbiol 10:2168

Matsumoto Y, Nagamachi T, Yoshikawa A, Yamazaki H, Yamasaki Y, Yamada T, Sugita T (2021) Development of an efficient gene-targeting system for elucidating infection mechanisms of the fungal pathogen *Trichosporon asahii*. Sci Rep 11:18270. https://doi.org/10.1038/s41598-021-97287-3

Mendes NS, Bitencourt TA, Sanches PR, Silva-Rocha R, Martinez-Rossi NM, Rossi A (2018) Transcriptome-wide survey of gene expression changes and alternative splicing in *Trichophyton rubrum* in response to undecanoic acid. Sci Rep 8:2520. https://doi.org/10.1038/s41598-018-20738-x

Monod M, Feuermann M, Salamin K, Fratti M, Makino M, Alshahni MM, Makimura K, Yamada T (2019) *Trichophyton rubrum* azole resistance mediated by a new ABC transporter, TruMDR3. Antimicrob Agents Chemother 63:e00863-e919. https://doi.org/10.1128/AAC

Peres NTA, Lang EAS, Bitencourt TA, Oliveira VM, Fachin AL, Rossi A, Martinez-Rossi NM (2022) The bZIP Ap1 transcription factor is a negative regulator of virulence attributes of the anthropophilic dermatophyte *Trichophyton rubrum*. Curr Res Microb Sci 3:100132. https://doi.org/10.1016/j.crmicr.2022.100132

Persinoti GF, de Aguiar Peres NT, Jacob TR, Rossi A, Vêncio RZ, Martinez-Rossi NM (2014) RNA-sequencing analysis of *Trichophyton rubrum* transcriptome in response to sublethal doses of acriflavine. BMC Genomics 15:S1. https://doi.org/10.1186/1471-2164-15-S7-S1

Reiss E, Shadomy HJ, Lyon GM (2011) Dermaatophytosis. In: Chambers KE (ed) Fundamental Medical Mycology. Wiley-Blackwell, Hoboken, pp 527–565

Reuß O, Vik Å, Kolter R, Morschhäuser J (2004) The SAT1 flipper, an optimized tool for gene disruption in *Candida albicans*. Gene 341:119–127. https://doi.org/10.1016/j.gene.2004.06.021

Roundtree TM, Juvvadi RP, Shwab KE, Cole CD, Steinbach JW (2020) *Aspergillus fumigatus* Cyp51A and Cyp51B proteins are compensatory in function and localize differentially in response to antifungals and cell wall Inhibitors. Antimicrob Agents Chemother. https://doi.org/10.1128/aac.00735-20.10.1128/aac.00735-20

Schuldiner M, Collins SR, Thompson NJ, Denic V, Bhamidipati A, Punna T, Ihmels J, Andrews B, Boone C, Greenblatt JF, Weissman JS, Krogan NJ (2005) Exploration of the function and organization of the yeast early secretory pathway through an epistatic miniarray profile. Cell 123:507–519. https://doi.org/10.1016/j.cell.2005.08.031

Smithies O, Gregg RG, Boggs SS, Koralewski MA, Kucherlapati RS (1985) Insertion of DNA sequences into the human chromosomal β-globin locus by homologous recombination. Nature 317:230–234. https://doi.org/10.1038/317230a0

Uchida K, Tanaka T, Yamaguchi H (2003) Achievement of complete mycological cure by topical antifungal agent NND-502 in guinea pig model of tinea pedis. Microbiol Immunol 47:143–146. https://doi.org/10.1111/j.1348-0421.2003.tb02797.x

Willger SD, Puttikamonkul S, Kim K-H, Burritt JB, Grahl N, Metzler LJ, Barbuch R, Bard M, Lawrence CB, Cramer RA Jr (2008) A sterol-regulatory element binding protein is required for cell polarity, hypoxia adaptation, azole drug resistance, and virulence in *Aspergillus fumigatus*. PLoS Pathog 4:e1000200

Xu X, Liu T, Yang J, Chen L, Liu B, Wang L, Jin Q (2018) The first whole-cell proteome- and lysine-acetylome-based comparison between *Trichophyton rubrum* conidial and mycelial stages. J Proteome Res 17:1436–1451. https://doi.org/10.1021/acs.jproteome.7b00793

Xu X, Hu X, Dong J, Xue Y, Liu T, Jin Q (2022) Proteome-wide identification and functional analysis of lysine crotonylation in *Trichophyton rubrum* conidial and mycelial stages. Front Genet. https://doi.org/10.3389/fgene.2022.832668

Yamada T, Makimura K, Hisajima T, Ito M, Umeda Y, Abe S (2008) Genetic transformation of the dermatophyte, *Trichophyton mentagrophytes*, based on the use of G418 resistance as a dominant selectable marker. J Dermatol Sci, 49:53–61. https://doi.org/10.1016/j.jdermsci.2007.08.009

Yamada T, Makimura K, Hisajima T, Ishihara Y, Umeda Y, Abe S (2009) Enhanced gene replacements in Ku80 disruption mutants of the dermatophyte, *Trichophyton mentagrophytes*. FEMS Microbiol Lett 298:208–217. https://doi.org/10.1111/j.1574-6968.2009.01714.x

Yamada Y, Maeda M, Alshahni MM, Monod M, Staib P, Yamada T (2014) Flippase (FLP) recombinase-mediated marker recycling in the dermatophyte *Arthroderma vanbreuseghemii*. Microbiology (n y) 160:2122–2135. https://doi.org/10.1099/mic.0.076562-0

Yamada T, Maeda M, Alshahni MM, Tanaka R, Yaguchi T, Bontems O, Salamin K, Fratti M, Monod M (2017) Terbinafine resistance of *Trichophyton* clinical isolates caused by specific point mutations in the squalene epoxidase gene. Antimicrob Agents Chemother 61:e00115-17. https://doi.org/10.1128/AAC.00115-17

Yamada T, Yaguchi T, Maeda M, Alshahni MM, Salamin K, Guenova E, Feuermann M, Monod M (2022) Gene amplification of CYP51B: a new mechanism of resistance to azole compounds in *Trichophyton indotineae*. Antimicrob Agents Chemother 66:e00059-22. https://doi.org/10.1128/aac.00059-22

Zhan P, Liu W (2017) The changing face of dermatophytic infections worldwide. Mycopathologia 182:77–86. https://doi.org/10.1007/s11046-016-0082-8

Zhang A, Lu P, Dahl-Roshak AM, Paress PS, Kennedy S, Tkacz JS, An Z (2003) Efficient disruption of a polyketide synthase gene (*pks1*) required for melanin synthesis through *Agrobacterium*-mediated transformation of *Glarea lozoyensis*. Mol Genet Genomics 268:645–655. https://doi.org/10.1007/s00438-002-0780-4

Zhang C, Gao L, Ren Y, Gu H, Zhang Y, Lu L (2021) The CCAAT-binding complex mediates azole susceptibility of *Aspergillus fumigatus* by suppressing SrbA expression and cleavage. Microbiologyopen 10:e1249. https://doi.org/10.1002/mbo3.1249

## Publisher's Note